

Structure and Dynamic Properties of Molten IVb-Te Mixtures around Eutectic Region

Yukinobu KAWAKITA, Kenji MARUYAMA¹ and Shin'ichi TAKEDA

Department of Physics, Faculty of Sciences, Kyushu University, Ropponmatsu, Fukuoka 810-8560, Japan

¹*Department of Chemistry, Faculty of Science, Niigata University, Niigata 950-2181, Japan*

Liquid binary mixture between Te and IVb elements have the eutectic region around 85 at. % Te. The viscosity for liquid Ge₁₅Te₈₅ has been reported to have strong temperature dependence above the melting temperature. To make clear the local structure around IVb and Te atoms, we have measured the neutron diffraction and EXAFS measurements for liquid Ge₁₅Te₈₅ and Sn₁₆Te₈₄ mixtures. The results for liquid Ge₁₅Te₈₅ mixture suggest that bonding state between Ge and Te decreases and becomes weak with increasing temperature rapidly, while the local structure of liquid Sn₁₆Te₈₄ doesn't show large temperature dependence. Large temperature dependence of physical properties of Ge₁₅Te₈₅ near the melting point can be understood by structural change from semiconducting chain to cluster of short chains.

KEYWORDS: neutron diffraction, EXAFS, structure, liquid Ge-Te

§1. Introduction

Many works on the electronic, thermodynamic and structural properties of Te-based liquid mixtures have been studied¹⁻⁶⁾ from the view point of compound forming effect at a certain composition, and the transition from a semi conducting to a metallic state with increasing temperature. Pure Te is known to form a two-fold coordinated chain structure even in the liquid state, and liquid Te shows metallic conductivity just above the melting point. This is explained by strong interchain coupling due to the thermal agitation, and the charge transfer from a lone pair orbital to an anti-bonding orbital on neighboring chains.^{7,8)} In the phase diagram of IVb-Te alloys, the eutectic region is found around 85 at. % Te. It is expected that local orderings between two fold coordinated structure of Te and cluster forming structure based on IVb-Te bond compete each other around the eutectic region.

The viscosity of liquid Ge₁₅Te₈₅ has large value just above the melting point and strong temperature dependence, while that of liquid Sn₁₆Te₈₄ does not have so strong temperature dependence.⁹⁾ In this paper, we present the neutron diffraction and EXAFS results for liquid Ge₁₅Te₈₅ and Sn₁₆Te₈₄ mixtures around the eutectic region and discuss bonding nature. The large temperature dependence of viscosity and anomalous behavior of thermodynamic quantities as near the melting point will be explained by structural change from semiconducting chain to cluster of short chains.

§2. Experimental Procedures

Samples were prepared by heating and mixing of elemental materials (Te; 99.999%, Ge; 99.9999%, Sn; 99.99%) in the quartz tube sealed under vacuum. Neutron diffraction measurements were carried out using the HIT-II spectrometer installed at KENS Neutron Scattering Facility in High Energy Accelerator Research Orga-

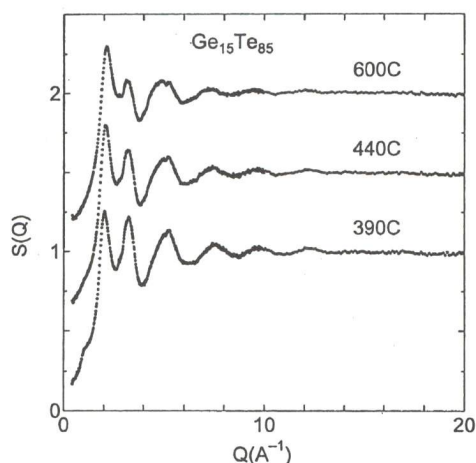


Fig.1. Temperature dependence of the total structure factors of liquid Ge₁₅Te₈₅.

nization, Tsukuba, Japan. Samples were put into a thin-walled (0.3mm) cylindrical cell made of fused silica with an inner diameter of 8mm. The sample was heated with a pair of infrared image heaters. Time-of-flight (TOF) spectra were taken for liquid Ge-Te system. The structure factors, $S(Q)$, in the range of momentum transfer Q up to 30 Å⁻¹ were deduced by the standard procedure⁷⁾ which includes the absorption correction, subtraction of scattering from the cell, normalization by using spectra for vanadium and reduction of multiple scattering contribution.

EXAFS measurements were carried out at the BL-10B station of the Photon Factory in KEK. Spectra at Ge, Te and Sn K-absorption edges were obtained in a transmission mode using a Si(311) monochromator.¹⁰⁾ The liquid samples were inserted into the gap between two X-ray windows made of quartz glass which were polished to be 0.3mm thickness. The optimum values of sample thickness, t , ranged from 40 μm to 200 μm.

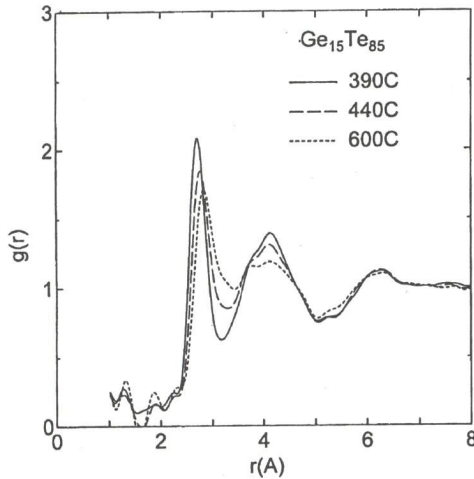


Fig. 2. Total pair distribution functions for liquid $\text{Ge}_{15}\text{Te}_{85}$.

§3. Results and Discussion

Figure 1 shows the structure factors, $S(Q)$, of liquid $\text{Ge}_{15}\text{Te}_{85}$ measured at 390 °C, 440 °C and 600 °C. A large temperature dependence is observed at the second peak around 3.2 \AA^{-1} of $S(Q)$. The oscillations decrease with increasing temperature at large wave number beyond 8 \AA^{-1} . The first peak of $S(Q)$ increases slightly with increasing temperature, and its position shifts to a higher Q region. A small but distinct prepeak can be observed around 1.0 \AA^{-1} at 390°C and it disappears with increasing temperature.

Figure 2 shows the pair distribution functions, $g(r)$, obtained by the Fourier transform of the interference function, $Q(S(Q)-1)$. The first peak of $g(r)$ decreases rapidly and shifts to a higher r direction with increasing temperature. The second distribution locating around 3.5 to 4.5 Å in the $g(r)$'s also reduces with increasing temperature.

Figure 3(a) shows the partial distribution functions, $F(r)$, extracted from the EXAFS signal for Ge K-edge in liquid $\text{Ge}_{15}\text{Te}_{85}$. The first peak in $F(r)$ appears smaller than the real bond length about $0.2 \sim 0.3 \text{ \AA}$ mainly because the phase shift has a negative k -dependence, nevertheless $F(r)$ is convenient to see a relative structural change. The first peak in $F(r)$ is located around 2.44 \AA at 400 °C. With increasing temperature up to 600 °C, it shifts to a longer r region by 0.1 \AA . The peak height decreases and becomes small rapidly above 450°C. Similar tendency can be observed in the $F(r)$ at Te K-edge. This suggests that a substantial change of local structure occurs in this liquid. Figure 3(b) shows the partial distribution function, $F(r)$, obtained from the EXAFS signal for Sn K-edge in liquid $\text{Sn}_{16}\text{Te}_{84}$. The temperature dependence is not so significant as that for liquid $\text{Ge}_{15}\text{Te}_{85}$. We have mentioned from EXAFS analysis of liquid $\text{Ge}_{15}\text{Te}_{85}$ that the coordination numbers of Te around Ge decreases from 2.6 at 400°C to 1.8 at 500°C with temperature raising only by 100°C and the Ge-Te bond elongates from 2.66 \AA at 400 °C to 2.73 \AA at 500 °C. This suggests that the bonding between Ge and Te becomes weak drastically and has more metallic character with increasing temperature. In fact, it is observed that viscosity of

liquid $\text{Ge}_{15}\text{Te}_{85}$ substantially decreases and conductivity increases in those temperature range.⁹⁾ The total structure factor of $\text{Ge}_{15}\text{Te}_{85}$ obtained from neutron diffraction includes three partial structures on Ge-Ge, Ge-Te and Te-Te pairs and their contributions in the total structure are 3.9%, 31.3% and 62.9%. Neumann *et al.* deduced the partial structure factors of Ge-Te and Te-Te pairs by both X-ray and neutron diffraction data, neglecting the Ge-Ge pairs in eutectic region.⁵⁾ Their results suggest that at a high temperature, Te-Te partial structure factor tends to resemble to the total structure factor of pure liquid Te just above the melting point.

To confirm structural change, numerical fitting has been done for the radial distribution function. The radial distribution function is calculated using the Te partial number density instead of the total number density as shown by full line in Figs. 4 and 5. When the first one and the incoherent contribution (1.9%) are neglected, it presents a linear combination of the partial radial distribution functions of Te atoms around the central Ge atom and Te atoms around the central Te atom. Assuming that the distribution of Ge-Te nearest neighbouring pairs is the same as one obtained from the analysis of Ge K-edge EXAFS data, structural information on the Te-Te covalent bonds and the further distributions was obtained by fitting a model function including several Gaussian functions and a non-correlated back ground,^{11,12)}

$$4\pi r^2 n_{\text{Te}} \frac{1}{2} \left(1 + \sin \left(\frac{\pi(r-R_{th})}{2R_w} \right) \right),$$

to the experimental radial distribution function, where $2R_w$ expresses the intermediate length between correlated and uncorrelated coordination and R_{th} indicates the threshold length. In this liquid R_h and R_w are taken as 4.83 \AA and 3.314 \AA , respectively. Each function is shown by dotted curves in the Figs 4 and 5. Gaussian curve fit analysis has been taken for radial distribution

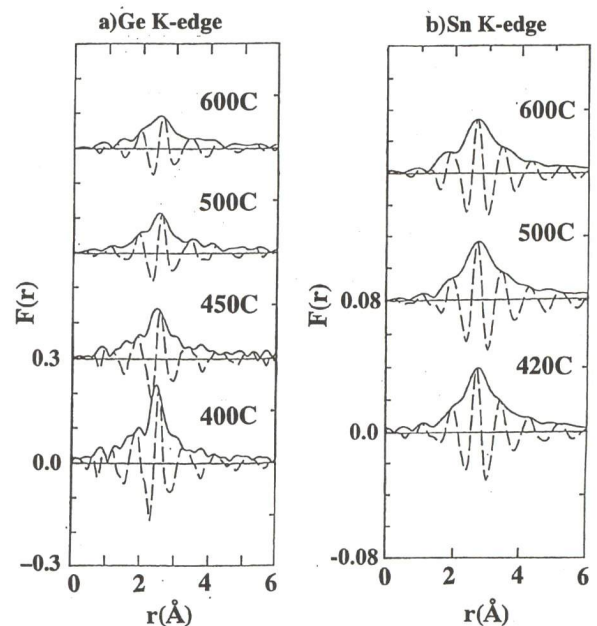


Fig. 3. Partial radial distribution function of liquid $\text{Ge}_{15}\text{Te}_8$ and liquid $\text{Sn}_{16}\text{Te}_{84}$.

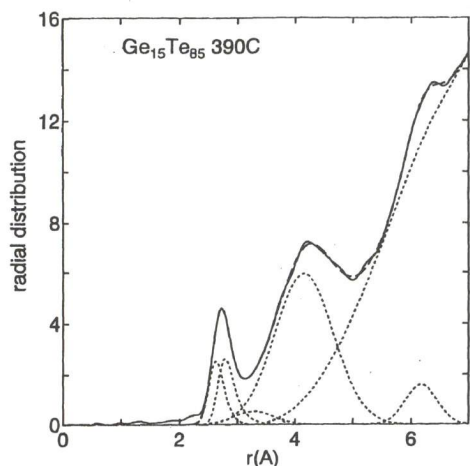


Fig. 4. Curve fitting of the radial distribution function for liquid $\text{Ge}_{15}\text{Te}_{85}$ at 390 °C.

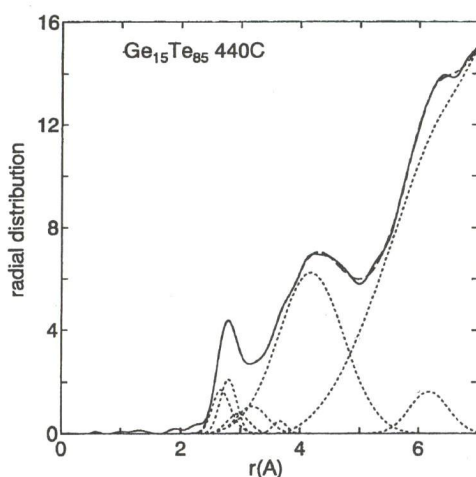


Fig. 5. Curve fitting of the radial distribution function for liquid $\text{Ge}_{15}\text{Te}_{85}$ at 440 °C.

function (RDF) based on the bond length and partial coordination from EXAFS measurements. For the low temperature liquid state at 390 °C, coordination of Ge-Te pairs are 2.756 at 2.667 Å and that of Te-Te pairs are 1.59 at 2.857 Å and one site fitting is good for Te-Te pairs. As for the RDF fitting at 440 °C, the coordination of Ge-Te pairs are obtained 2.09 at 2.707 Å, however, one site fitting is not good for the Te-Te pairs and two sites are required for Te-Te pairs to get good fitting results, and shortens bonds of Te-Te pairs result in 1.13 at 2.798 Å and slightly longer one become 1.03 at 3.193 Å. The fitting results can be interpreted in the similar way to the case of pure liquid Te, which shows structural change from selenium-like semiconducting chain to cluster of short chains strongly interacting each other.⁷⁾ With increasing temperature from the supercooled liquid region, the length of the Te chain shorten by thermal agitation and fraction of Te atoms at the chain end

becomes larger.⁷⁾ Chain end is charged negatively and introduces large charge fluctuation in the Te chain. Such charge fluctuation generates inter-chain interaction binding short chains each other. The inter-chain interaction stimulates charge transfer among neighbouring chains, especially charge transfer from the lone pair orbital of Te atom to the anti-bonding orbital of the neighbouring chain, which strengthens chain coupling by charge fluctuation. This microscopic model^{7,8)} can explain every anomaly near the melting point, that is, volume contraction by inter-chain coupling, large heat capacity by structural change from semiconducting regime to metallic regime, metallic conduction between neighbouring chains by delocalization of lone pair orbital. The fitting results in Fig. 5 suggests that such strong inter-chain interaction exists even in the liquid $\text{Ge}_{15}\text{Te}_{85}$.

§4. Conclusions

The results of neutron diffraction and EXAFS measurements for liquid $\text{Ge}_{15}\text{Te}_{85}$ mixture and liquid $\text{Sn}_{16}\text{Te}_{84}$ mixture have been presented. The large temperature dependence has been observed for liquid $\text{Ge}_{15}\text{Te}_{85}$ with increasing temperature just above the melting point.

The large temperature dependence of viscosity just above the melting point and anomalous behavior of thermodynamic quantities as molar volume and sound velocity near the melting point can be understood by structural change from semiconducting chain to cluster of short chains. Since the length of the chains will be shortened by thermal agitation, the fraction of Te atoms at the chain end will increase and such Te generates the charge fluctuation in the Te chain. Such charge fluctuation generates the inter-chain interaction and also the every anomaly near the melting point. This will explain every anomalous behavior of Te based alloys near the melting point.

- 1) J. E. Enderby and A. C. Barnes: Rep. Prog. Phys. **53** (1990) 85, M. Cutler: Liquid Semiconductors (Academic Press, 1977).
- 2) J.C. Valiant and T.E. Faber: Phil. Mag. **26** (1974) 571.
- 3) S. Takeda and Y. Tsuchiya: J. Phys. Soc. Jpn. **47** (1979) 109.
- 4) T. Aakasofu, S. Takeda and S. Tamaki: J. Non-Cryst. Solids **59 & 60** (1983) 1075.
- 5) H. Neumann, W. Hoyer, W. Matz and M. Wobst: J. Non-Cryst. Solids **97-98** (1987) 1251.
- 6) Y. Tsuchiya: J. Phys. Soc. Jpn. **60** (1991) 227.
- 7) Y. Kawakita, M. Yao and H. Endo: J. Phys. Soc. Jpn. **66** (1997) 1339.
- 8) Y. Kawakita, S. Yoshioka, I. Hiraishi, M. Kanehira and S. Takeda: Jpn. J. Appl. Phys. **38-1** (1999) 472.
- 9) H. Neumann, F. Herwig and W. Hoyer: J. Non-Cryst. Solids **205** (1996) 438.
- 10) S. Yoshioka, Y. Kawakita, M. Kanehira and S. Takeda: Jpn. J. Appl. Phys. **38-1** (1999) 468.
- 11) M. Misawa: J. Phys. Condens Matter **4** (1992) 4491.
- 12) M. Yao and H. Endo: J. Non-Cryst. Solids **205-207** (1996) 85.